

Fracture Toughness to Understand Stretch-Flangeability and Edge Cracking Resistance in AHSS



DANIEL CASELLAS, ANTONI LARA, DAVID FRÓMETA, DAVID GUTIÉRREZ, SÍLVIA MOLAS, LLUÍS PÉREZ, JOHANNES REHRL, and CLEMENS SUPPAN

The edge fracture is considered as a high risk for automotive parts, especially for parts made of advanced high strength steels (AHSS). The limited ductility of AHSS makes them more sensitive to the edge damage. The traditional approaches, such as those based on ductility measurements or forming limit diagrams, are unable to predict this type of fractures. Thus, stretch-flangeability has become an important formability parameter in addition to tensile and formability properties. The damage induced in sheared edges in AHSS parts affects stretch-flangeability, because the generated microcracks propagate from the edge. Accordingly, a fracture mechanics approach may be followed to characterize the crack propagation resistance. With this aim, this work addresses the applicability of fracture toughness as a tool to understand crack-related problems, as stretch-flangeability and edge cracking, in different AHSS grades. Fracture toughness was determined by following the essential work of fracture methodology and stretch-flangeability was characterized by means of hole expansions tests. Results show a good correlation between stretch-flangeability and fracture toughness. It allows postulating fracture toughness, measured by the essential work of fracture methodology, as a key material property to rationalize crack propagation phenomena in AHSS.

DOI: 10.1007/s11661-016-3815-x

© The Minerals, Metals & Materials Society and ASM International 2016

I. INTRODUCTION

CUTTING or shearing operations are widely used in metal sheet forming industries to produce final components. It is well known that cut or sheared edges may present damage in terms of surface irregularities, microvoids and microcracks. The degree of such damage at the cut edge is known as edge integrity. It is known to influence part quality in materials with limited ductility when sheared edges are subjected to bending or stretching in subsequent forming operations. This is the case for the so-called advanced high strength steels (AHSS) that are extensively implemented in the automotive industry to reduce weight and increase crashworthiness (a modern vehicle body contains about 30-50 pct of AHSS^[1]).

Although AHSS have contributed to the huge improvement of today's vehicles, they have also introduced new challenges which are still only solved partially. In the last years, many works focused on springback and formability prediction of these steels.^[2-6] However, less attention has been given to the cracking phenomena observed for some AHSS grades at cut or sheared edges (Figure 1). Edge cracking is associated with sheared areas that expands during forming operations involving stretch flanging or hole expansion. This process increases the flange edge length during the deformation.^[7] Typical examples of stretch flanges in the automotive industry include cut-outs in automotive inner panels and corners of window panels, hub-holes of wheel disks, hidden joints, *etc.* Edge cracking compromises part quality and it is a serious production problem, because if it is not accounted for in the overall design, the load paths through the vehicle frame in a crash situation can be misdirected and the resultant intrusion levels can exceed target levels. Such problem was not observed in mild steels, whose high ductility prevents the cut edge from cracking, and less knowledge and expertise are available to immediately solve it in industrial parts.^[8,9]

AHSS are more sensitive to the crack edge integrity, so their crack edge resistance depends on the hole preparation method (punching, laser cutting waterjet cutting...), as well as on the steel microstructure to tolerate the induced damage.^[10-12] Hence, the edge fracture can be considered as a high risk for AHSS automotive components. The traditional approaches, such as the forming limit diagram (FLD), are unable to

DANIEL CASELLAS, Director of Materials Technology Area, is with Fundació CTM-Centre Tecnològic, Plaça de la Ciència 2, 08243 Manresa, Spain, and also with Luleå University of Technology, 971 87 Luleå, Sweden. Contact e-mail: Daniel.casellas@ctm.com.es ANTONI LARA, DAVID FRÓMETA, and SÍLVIA MOLAS, Researchers at Materials Technology Area, are with Fundació CTM-Centre Tecnològic. DAVID GUTIÉRREZ, formerly Ph.D. Student with Fundació CTM-Centre Tecnològic, is now R&D Manager with Vac-tron S.A., C. Joan de la Cierva 6, 08420 Canovelles, Spain. LLUÍS PÉREZ, formerly Junior Researcher with Fundació CTM-Centre Tecnològic, is now Ph.D. Student with IUC Olfström, Vällaregatan 30, 293 38 Olofström, Sweden. JOHANNES REHRL and CLEMENS SUPPAN, Researchers, are with Voestalpine Stahl GmbH, Voestalpine-Straße 3, 4020 Linz, Austria.

Manuscript submitted October 10, 2013.

Article published online October 20, 2016

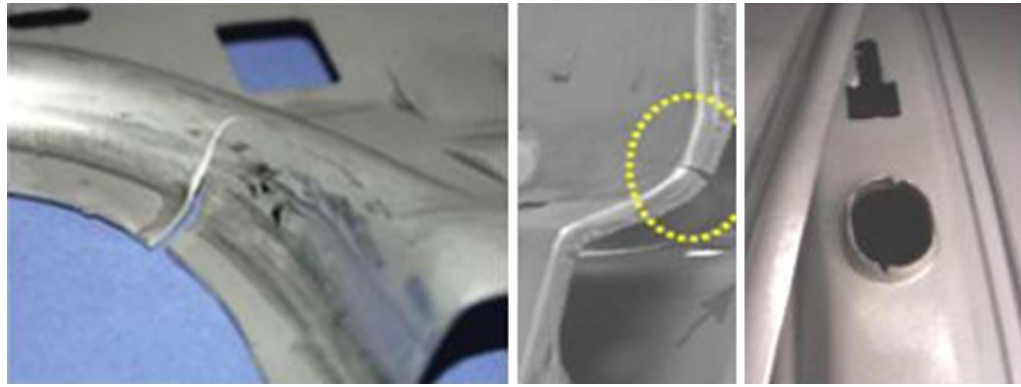


Fig. 1—Cracks produced in cold formed AHSS automotive parts.

Table I. Chemical Composition, in Weight Percent

Steel Grade	C	Si	Mn	Cr	B	Al
CP1000	~0.1	<0.5	1.8–2.2	<0.7	<0.003	—
DP1000	~0.15					
TBF	~0.2	0.5–1.0	2.2–2.6			
Q&P	~0.1					
TBF/Q&P	~0.1					
PHS1500	~0.2	~0.2	~1.2		~0.003	
PHS1000						

predict this type of fracture and great efforts have been made to develop failure criteria that could predict edge fracture.^[9] In this sense, stretch-flangeability has become a particularly important formability parameter in addition to tensile properties, especially for parts under heavy deformation conditions, to rationalize edge cracking problems.

The stretch-flangeability in low C Steels and AHSS has been studied well, but the results obtained in some AHSS grades were initially surprising, since stretch-flangeability increases when the material strength also increases and ductility diminishes.^[6,11,13] This observation is in the opposite way of thinking for ductile steels, where it is accepted that ductility improves flangeability. In dual-phase steels, this behavior is explained by the hardness difference between ferrite and martensite.^[14–16] On the other hand, the works of Fonstein *et al.*^[17] and Takahashi *et al.*^[18] approached the problem from a fracture mechanics point of view and proposed that fracture toughness can be used to rationalize the observed behavior for AHSS. However, this approach is not intensively applied to metal sheets yet because fracture toughness cannot be readily measured by standard characterization techniques. It means that fracture or crack propagation phenomena in metal sheets, as the observed behavior in stretch-flangeability tests, cannot be rationalized in terms of intrinsic mechanical properties, which hampers process and material optimization. Aimed at filling this gap of knowledge, the objective of the present work is to measure and use fracture toughness as a tool to understand crack-related problems in AHSS sheets, as stretch-flangeability or edge cracking resistance.

II. MATERIALS AND EXPERIMENTAL PROCEDURE

A. Materials

Different AHSS grades were studied: (a) two commercially available cold forming grades, a dual-phase steel (DP1000) and a complex phase steel (CP1000); (b) three 3rd generation AHSS grades: Trip-aided Bainitic Ferrite (TBF) steel, Quenching & Partitioning (Q&P) steel, and mixed TBF/Q&P microstructure; (c) two microstructures of hot stamped boron steel: one in press hardened condition, named as PHS1500 and another one with an additional tempering treatment, named as PHS1000.

Table I shows the chemical composition of the investigated steels. Microstructure of these steel grades has been studied by means of scanning electron microscopy (SEM) after electro-polishing. The corresponding microstructures are in Figures 2, 3, and 4. CP-like grades (CP1000 and mixed TBF/Q&P) as well as the Q&P grade show a homogeneous matrix of bainite/tempered martensite. Q&P and mixed TBF/Q&P also contain retained austenite. In DP1000 and TBF grades, the matrix consists of a mixture of ferrite, bainitic ferrite, bainite/tempered martensite, martensite and retained austenite. PHS1500 consists of a homogeneous martensitic matrix, which is slightly auto-tempered during cooling. The tempering treatment for PHS1000 basically leads to relaxation of the tetragonal martensite lattice by formation of carbides, which can be observed as white lines and spots in Figure 4(b).

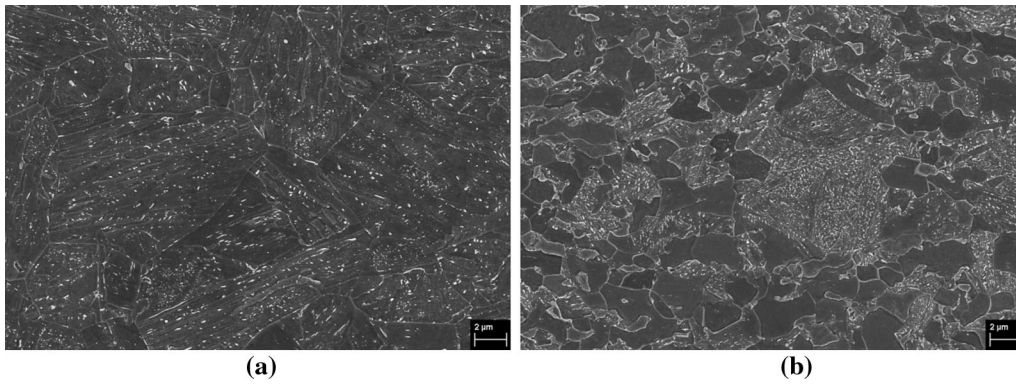


Fig. 2—Microstructure of: (a) CP1000 steel and (b) DP1000 steel.

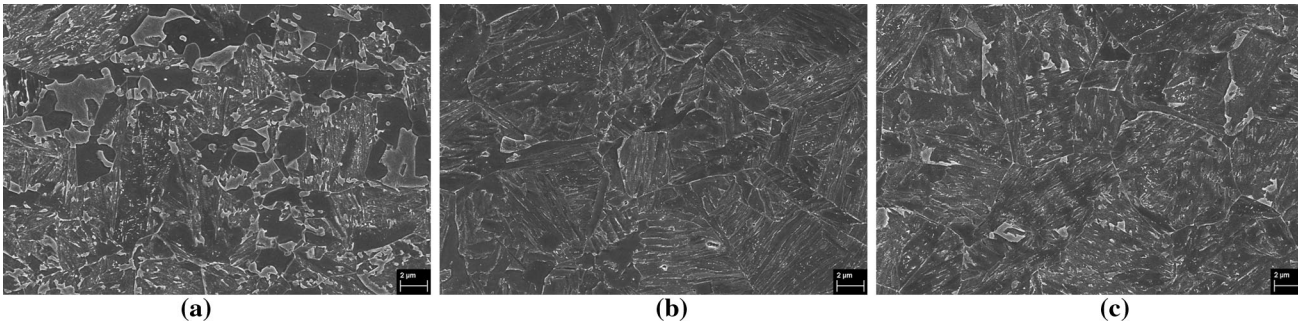


Fig. 3—Microstructure of 3rd generation AHSS: (a) TBF, (b) Q&P, and (c) TBF/Q&P grade.

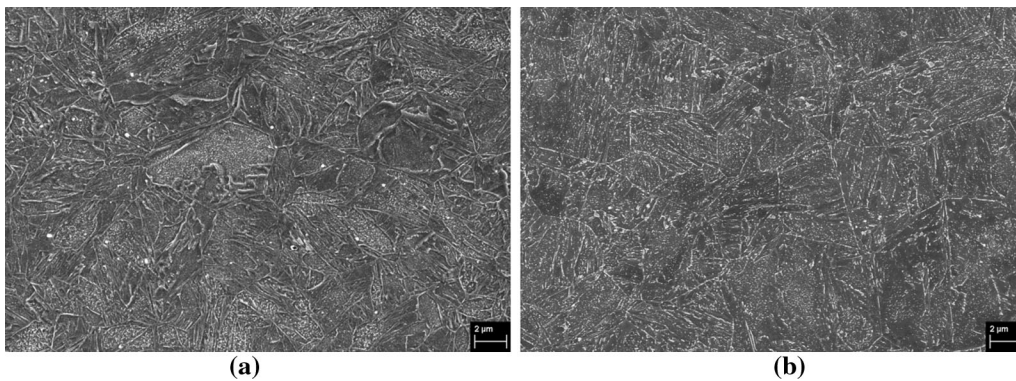


Fig. 4—Microstructure of press hardened steels: (a) PHS1500, (b) PHS1000.

B. Tensile Tests

Conventional axial tensile tests were performed according to EN-ISO6892-1 with the specimens oriented transversally to the rolling direction. Table II shows the results.

C. Hole Expansion Test

Looking at stretch-flangeability, the hole expansion test (HET) closely resembles the process under production conditions to form such flanges starting with punched holes. This is the most used method to evaluate the suitability of the sheet steel for forming such

“flanges.” The value obtained in this test is the hole expansion ratio (HER), which is calculated using the initial hole diameter (D_0) and the diameter at first through-thickness crack apparition (D_h) as follows:

$$\text{HER(pct) or } \lambda = \left[\frac{D_h - D_0}{D_0} \right] \times 100. \quad [1]$$

HER indicates the maximum diametrical expansion that a circular punched hole can reach when a conical tool is forced into it until a crack in the hole edge extends through the full sheet thickness. The HET were carried out in a universal testing machine using a conical

Table II. Mechanical Properties: Yield Strength (YS), Ultimate Tensile Strength (UTS), Total Elongation and Hardening Exponent (n)

Steel Grade	t (mm)	YS (MPa)	UTS (MPa)	Elongation (pct)	n
CP1000	1.4	920	1008	8.8	0.05
DP1000	1.4	738	1027	10.3	0.10
TBF	1.5	725	1019	14.7	0.12
Q&P	1.4	909	1209	7.4	0.09
TBF/Q&P	1.4	876	1026	11.3	0.09
PHS1500	1.5	1075	1552	5.2	0.08
PHS1000	1.5	988	1007	7.3	0.05

Thickness (t) for all grades is also given.

punch with an angle of 60deg according to ISO16630 standard.^[19] The initial hole diameter was 10 mm, and the driving speed of the conical punch was 1 mm/s. The punching clearance was set to 12 pct, because it is following standard recommendations and previous work where it is experimentally assessed that this value gives rise to the maximum HER in AHSS.^[11] The followed punching and flanging processes are shown in Figure 5. Three samples of 100 × 100 mm from each steel were tested. A clamping force of 50 KN was applied to the test piece to prevent any material draw-in from the clamping area during the test. During the HET, the nucleation and extension of cracks were detected by a digital image correlation equipment (DIC) located below the tool. D_h was measured from the image at which the first through-thickness crack was observed, before removing the punch.

D. Measurement of Fracture Toughness in Thin Sheets

In fracture mechanics, the fracture toughness is defined as the energy spent in the creation of two surfaces at the crack tip that give rise to crack propagation. For ductile materials, experimental approaches based on elastic-plastic fracture mechanics allow determining the crack propagation resistance, as the J -integral (giving the value of J_C), the J - R curve or the CTOD measurement. The experimental complexity of standardized methods and the difficulty for transferring the obtained values to thin sheet components have given rise to a lack of knowledge regarding toughness of metal sheets. As a consequence, the fracture toughness of the AHSS sheets is not known. For thin plates, an alternative method to characterize fracture toughness was developed in the 80s; the EWF (Essential Work of Fracture) methodology. It was successfully applied to characterize ductile alloys, and the obtained toughness value was found to be equivalent to J_C by many authors.^[20–27] Nowadays, it is commonly applied to characterize polymeric thin films following a protocol developed by the European Structural Integrity Society (ESIS), but it is not extensively used for thin steel sheets. Recent works show that the EWF methodology can be applied to AHSS sheets.^[27–31]

The EWF is experimentally evaluated by following the methodology developed by Cotterell and Reddel.^[20] These authors proposed that the total work of fracture

(W_f) during the ductile fracture can be separated into two components: (i) The essential work of fracture (W_e) spent in the fracture process zone (FPZ) in front of the crack tip, and (ii) non-essential plastic work (W_p) dissipated in an outer region as a consequence of plastic deformation. Double-edge-notched tensile (DENT) specimen (Figure 6) is particularly suitable for fracture mechanics tests because the transverse stress between the notches is tensile and there is no buckling. In DENT specimens if the material in front of the crack tip of the two notches, the ligament, is completely yielded and the plastic zone is confined to the notched ligament, then the plastic work performed for total fracture is proportional to the plastic volume at crack imitation and the work performed at the FPZ is proportional to the fractured area. It can be expressed as

$$W_f = W_e + W_p = w_e l t + w_p \beta^2 t, \quad [2]$$

where β is a shape factor that depends on the shape of the plastic zone, t is the sheet thickness, and l is the ligament length between the two notches. The specific work of fracture (w_f) is obtained by dividing Eq. [2] by the initial ligament area $l t$. Thus, Eq. [2] can be rewritten as

$$\frac{W_f}{l t} = w_f = w_e + w_p \beta l. \quad [3]$$

If w_f is plotted against the ligament length l , a straight line with a positive intercept, which is the specific essential work of fracture (w_e), is obtained.

When applying the EWF methodology to metal sheets, it should be kept in mind that the obtained values of w_e are greatly affected by the notch root radius. Such effect has been experimentally demonstrated in mild and dual-phase steels.^[30,31] The effect of the notch root radius on the fracture toughness measurement is well known in plain strain fracture toughness tests, below a critical notch root radius value the fracture toughness measurements are independent of the notch radius and fracture toughness is considered as a material intrinsic property. To avoid the effect of notch root radius, the ASTM E399 procedure for evaluating the fracture toughness suggests the nucleation of a fatigue crack at the notch root. This fatigue crack has the lowest possible radius at the crack tip, ensuring valid fracture

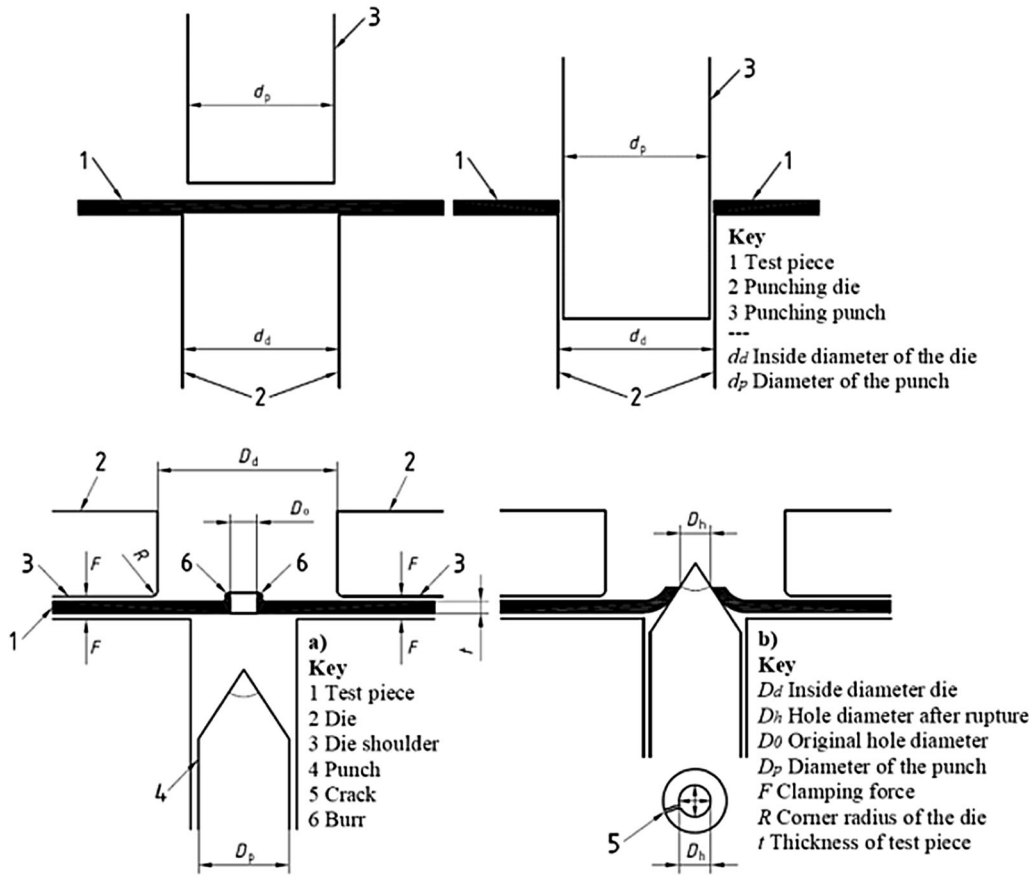


Fig. 5—Hole punching and hole expansion procedure followed in this work according to ISO16630.^[19]

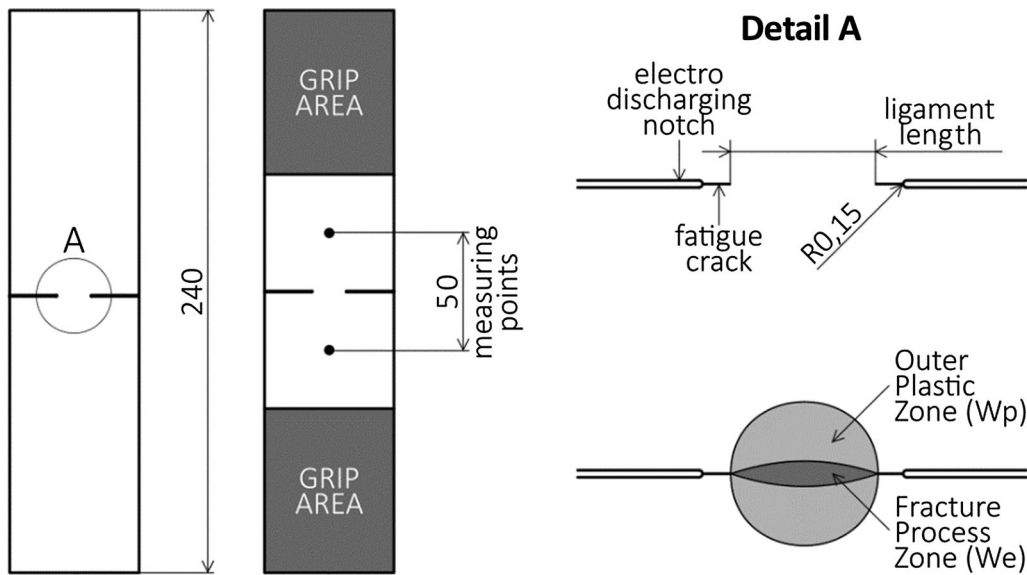


Fig. 6—Double-edge-notched specimen (DENT) indicating the fracture and plastic zone.

toughness values. Similarly, in the EWF methodology, notches with the lowest possible root radius must be used (Figure 6). However, w_e is not fully a material intrinsic property because it is influenced by necking of the fracture process zone and this in turn depends on the thickness of the sheet material.

In the present work, W_f was measured by loading DENT specimens of 240×55 mm, extracted transversally to the sheet rolling direction, in a universal testing machine with a speed of 1 mm/min. The displacement was measured with a video extensometer with gauge length of 50 mm. Specimens ligaments length ranges

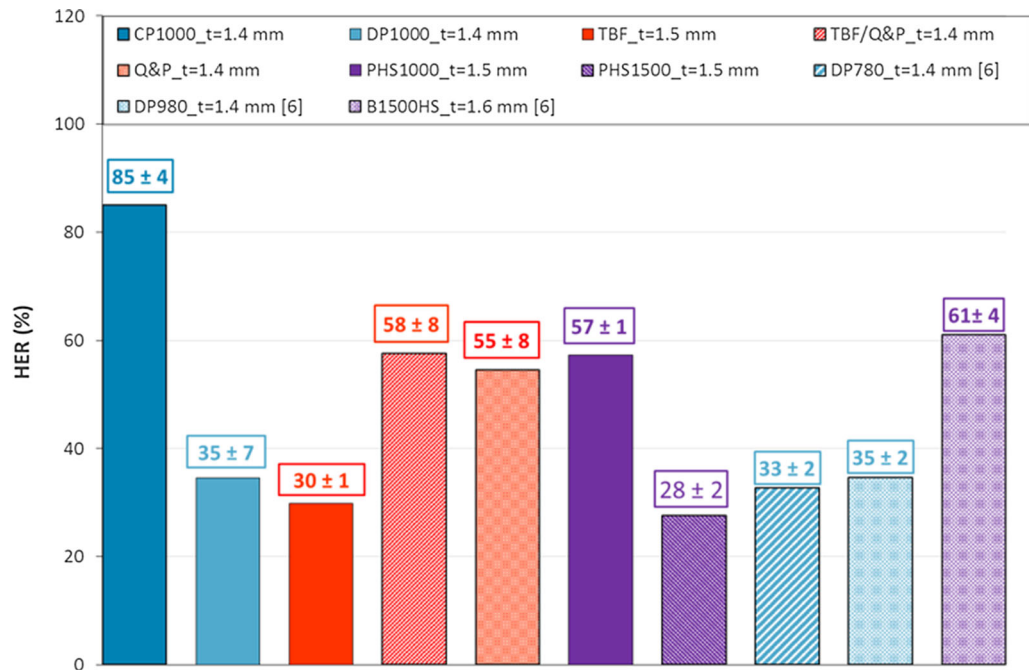


Fig. 7—HER values of the investigated steels, together with reported results for other AHSS.^[6]

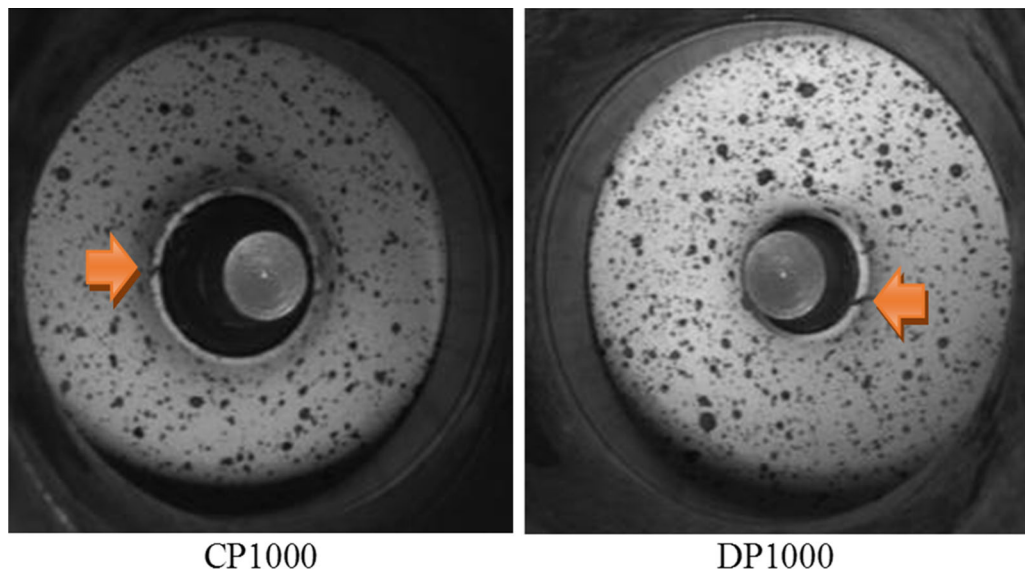


Fig. 8—First crack extension in the hole edge of CP1000 and DP1000 steels (orange arrows).

from 6 to 16 mm. About 3 to 5 specimens were tested up to fracture for each ligament length. The plot of w_f against l gives the values of w_c , as detailed before. Linear fitting was performed using a confidence interval of 95 pct.

III. RESULTS

A. Hole Expansion Test

Figure 7 shows the measured HER values. They are similar to previously reported results for other AHSS, as

DP780, DP980 and press hardened steels.^[6] They are also considerably lower than those obtained with mild steels, where HER ranges from 100 to 140 pct.^[6,30,32] HER values show relatively large scatter, as has been reported by other authors in AHSS.^[6,33] Figure 8 shows pictures of the first crack extension around the flange in DP1000 and CP1000 steels determined with the DIC technique. From Figure 8, the poor hole expansion of DP1000 before the first crack extension can be seen, whilst CP1000 steel presents a much greater hole expansion capacity than the DP steel. As expected CP-like microstructures as those in CP, Q&P, PHS1000

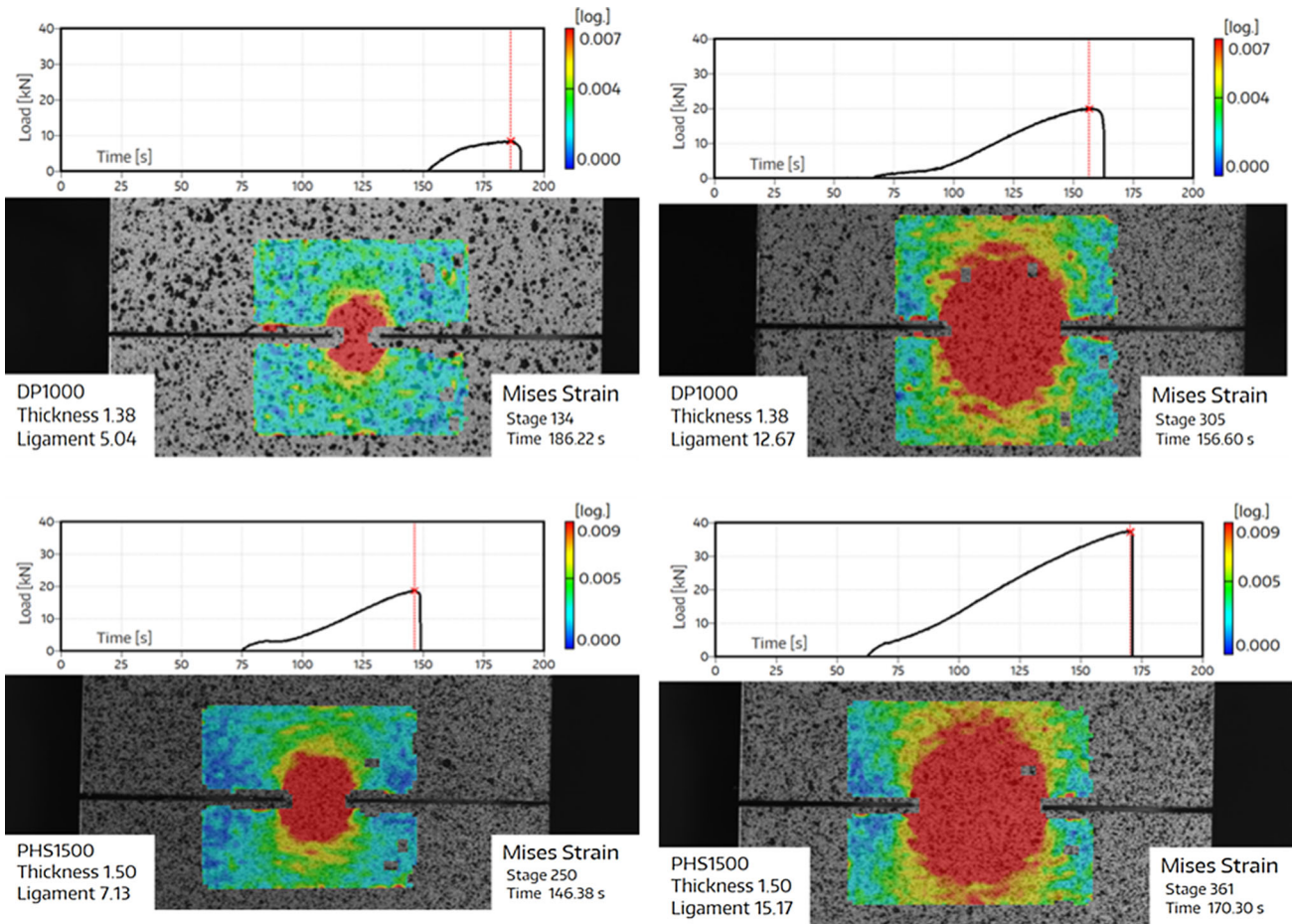


Fig. 9—Strain analysis on DP1000 and PHS1500. At maximum load the ligament area is fully yielded. DIC images show in red the material area over the yield stress.

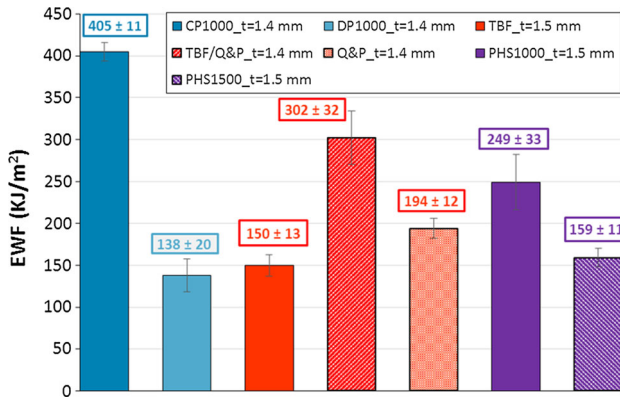


Fig. 10— w_e values obtained from the investigated steels.

and TBF/Q&P show high HER values, meanwhile DP-like microstructures, as DP and TBF, show low HER values. It is in agreement with previous works on multiphase steels, containing mixtures of ferrite, bainite and martensite, as CP and DP. In such steels, the combination of a soft phase, ferrite, with a hard phase, martensite or bainite, gives rise to high strain hardening coefficients and large ductility. Damage in DP and CP steels is related to the hardness difference between

phases. Strain localizes in ferrite and promotes void generation at the ferrite/martensite interface. Thus, finer microstructures as well as replacement of martensite by bainite give rise to higher damage-resistant microstructures and show higher HER values.^[15–18] PHS1500 presents the lowest HER values because the microstructure is martensite, with lower damage resistance than DP and CP ones.

B. Essential Work of Fracture

The definition of the EWF methodology imposes that the crack tip must be yielded before the onset of crack propagation. In DENT specimens, it means that the material between the two notches must be fully yielded. This constraint is satisfied in mild steels,^[26] but the higher yield strength of AHSS implies that this condition must be verified for the studied AHSS. DIC analysis was performed for all the steels studied and showed that at maximum load in samples with the largest ligament length, the ligament area is fully yielded and that the plastic zone morphology is almost circular. Both requirements must be fulfilled to obtain valid values of w_e from Eq. [3]. Figure 9 shows DIC analysis on the shortest and largest ligament for DP1000 and PHS15000. The measured values of w_e are shown in Figure 10.

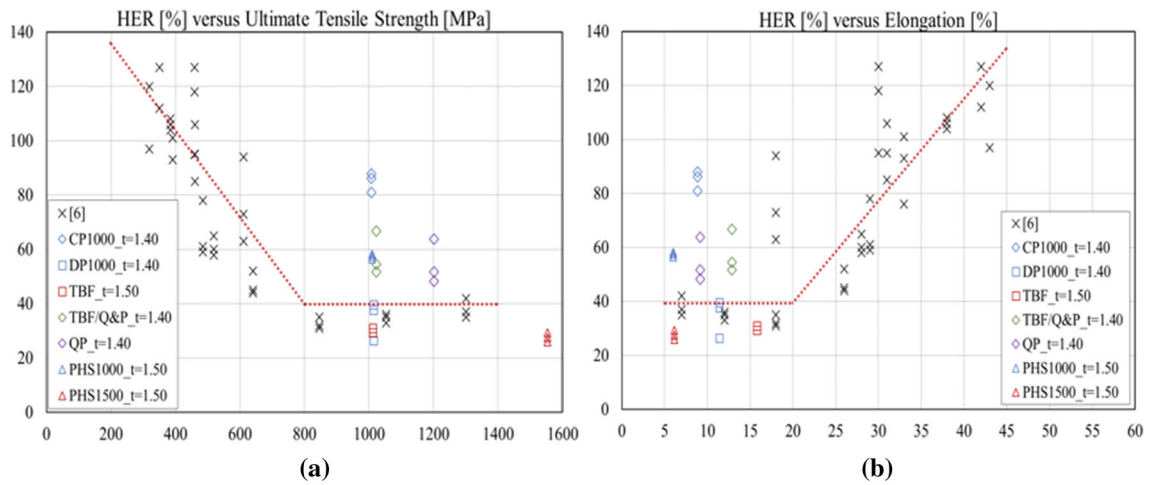


Fig. 11—Correlation between HER and mechanical properties of AHSS and new generation steels, together with published data for mild steel and AHSS^[6]: (a) Correlation between HER and ultimate tensile strength. (b) Correlation between HER and elongation.

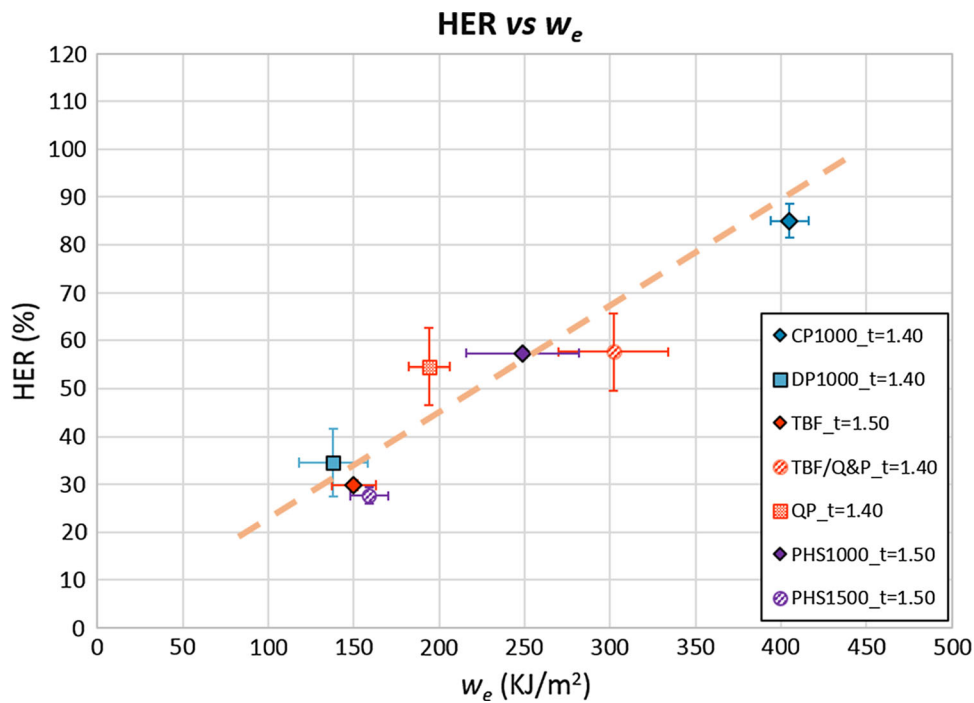


Fig. 12—Correlation between HER and EWF of AHSS and new generation steels.

Similarly to the HER results, a relationship between microstructure and toughness can be seen; CP-like grades (CP1000, TBF/Q&P, and Q&P grades) show higher EWF values than DP-type steels (DP1000 and TBF). PHS1500 presents also one of the lowest toughness values, a value which increases significantly after the tempering treatment done at PHS1000.

IV. DISCUSSION

Figure 11(a) shows the relationship between HER and tensile strength for the studied steels, together with results

for mild steels and other AHSS grades extracted from Reference 6. Results for mild steel and AHSS with tensile strength lower than 800 MPa show an almost linear correlation between HER and tensile strength and elongation, so HER linearly decreases when tensile strength increases. When HER values are plotted against elongation, the opposite trend is observed (Figure 11(b)). However, such relationships are not followed by the here investigated AHSS grades, with tensile strength above 800 MPa. This experimental behavior is in agreement with previous works for AHSS, where it is stated that ductility or elongation cannot be used to rationalize stretch-flangeability in AHSS.^[13,14,34,35]

Stretch-flangeability is dictated by the propagation of cracks through the material thickness; thus, the HET values could be related to the material resistance to crack propagation, which is the fracture toughness. Fonstein *et al.*^[17] and Takahashi *et al.*^[18] also stated that stretch-flangeability is controlled by the propagation of cracks or defects introduced during hole cutting and showed that tougher materials (measured in terms of J_{IC}) give rise to higher HER values. Aimed at proving such correlation, the results of EWF have been used to rationalize the HER values in the current work. It is shown in Figure 12. The experimental values of HER and w_e correlate very well and fits an almost linear relationship, *i.e.*, the tougher materials present higher HER values, whilst lower HER ones are associated with lower w_e . Accordingly, fracture toughness of AHSS sheets, in terms of w_e , can be used to properly rationalize stretch-flangeability in AHSS. These results allow to postulate that fracture toughness becomes a relevant material property when designing AHSS with improved edge cracking resistance.

V. CONCLUSIONS

Based on the experimental results of stretch-flangeability and fracture toughness measurements performed by means of the EWF methodology for several grades of AHSS with high tensile strength, the following conclusions can be drawn:

- The EWF methodology can be applied to AHSS sheets with very high tensile strength, up to 1500 MPa, to estimate the fracture toughness.
- Classical mechanical properties, such as ultimate tensile strength and elongation, are unable to predict HER in AHSS with high tensile strength (above 800 MPa).
- The values of fracture toughness, in terms of w_e , show the same trend as stretch-flangeability for the investigated steels.
- Fracture toughness is the material property to rationalize the observed improvement of stretch-flangeability for some AHSS microstructures. Furthermore, fracture toughness may help to understand the cracking-related phenomena in AHSS, as edge cracking.

ACKNOWLEDGMENTS

This investigation has been partially funded by the Catalan government under Grant TECCTA-13-1-0005 and by the European Commission, Research Fund for Coal and Steel, under Grant Agreement RFSR-CT-2014-00015 (Tough-Sheet).

REFERENCES

1. N. Lutsey: *Report UCD-ITS-RR-10-10*, Institute of Transportation Studies, University of California, Davis, CA, 2010.
2. P. Chen and M. Koç: *J. Mat. Proc. Technol.*, 2007, vol. 190, pp. 189–98.
3. P. Tsiouridis, E. Werner, C. Kremaszky, and E. Trag: *Steel Res. Int.*, 2006, vol. 77, pp. 654–67.
4. P.J. Jacques: *Curr. Opin. Solid State Mater. Sci.*, 2004, vol. 8, pp. 259–65.
5. A. Karelova, C. Kremaszky, M. Dünckelmeyer, E. Werner, T. Hebesberger, A. Pichler: *Mat. Sci. Tech. (MS&T)*, 2009, pp. 1358–68.
6. X. Chen, H. Jiang, Z. Cui, C. Lian, and C. Lu: *Proc. Eng.*, 2014, vol. 81, pp. 718–23.
7. V. Uthaisangsuk, U. Prahll, and W. Bleck: *Comput. Mat. Sci.*, 2009, vol. 3, pp. 617–23.
8. X. Wu, H. Bahmanpour, and K. Schmid: *J. Mat. Proc. Technol.*, 2012, vol. 212, pp. 1209–24.
9. M. Luo and T. Wierzbicki: *Int. J. Solids Struct.*, 2010, vol. 47, pp. 3084–102.
10. D.J. Thomas: *J. Fail. Anal. Preven.*, 2013, vol. 13 (4), pp. 451–62.
11. D. Gutiérrez, J. Escaler, A. Lara, D. Casellas, J.M. Prado: *Proceedings of the IDDRG2011*.
12. K. Watanabe, M. Tachibana, K. Koyanagi, K. Motomura: *LS-Dyna Conference*, 2006.
13. P. Larour, H. Pauli, J. Freudenthaler, A. Grünsteidl: *Proceedings of the IDDRG2011*.
14. X. Fang, Z. Fan, B. Ralph, P. Evans, and R. Underhill: *J. Mater. Sci.*, 2003, vol. 38, pp. 3877–82.
15. K. Hasegawa, K. Kawamura, T. Urabe, and Y. Hosoya: *ISIJ Int.*, 2004, vol. 44, pp. 603–09.
16. G. Avramovic-Cingaraa, Y. Ososkova, M.K. Jain, and D.S. Wilkinson: *Mater. Sci. Eng. A*, 2009, vol. 516, pp. 7–16.
17. N. Fonstein, H-J. Jun, G. Huang, S. Sriram, B. Yan: *Mater. Sci. Technol.* 2011, pp. 634–41.
18. Y. Takahashi, O. Kawanom, K. Ushiodam, S. Aihara: *Asia Steel Int. Conference*, 2012.
19. *ISO/TS16630*. Metallic materials – Method of hole expanding test, 2003.
20. B. Cotterell and J.K. Reddel: *Int. J. Fracture*, 1977, vol. 13, pp. 267–77.
21. Y.W. Mai and P. Powell: *J. Polym. Sci.*, 1991, vol. 29, pp. 785–93.
22. B. Cotterell and A.G. Atkins: *Int. J. Fract.*, 1996, vol. 81, pp. 357–72.
23. J. Wu and Y.W. Mai: *Polym. Eng. Sci.*, 1996, vol. 36, pp. 2275–88.
24. Y. Marchal, K. Schmidt, T. Pardoën, R. Knockaert, I. Doghri: *ECF 11. Mechanisms and Mechanics of Damage and Failure*, 1996, pp. 2259–65.
25. T. Pardoën, Y. Marchal, and F. Delannay: *J. Mech. Phys. Solids.*, 1999, vol. 47, pp. 2093–123.
26. T. Pardoën, F. Hachez, B. Marchioni, P.H. Blyth, A.G. Atkins: *J. Mech. Phys. Solids*, 2004, vol. 52, pp. 423–52.
27. G. Lacroix, T. Pardoën, and P.J. Jacques: *Act. Mat.*, 2008, vol. 56, pp. 3900–13.
28. R. Muñoz, A. Lara, D. Casellas: *Proceedings of the IDDRG2011 International Conference*, 2011.
29. D. Gutiérrez, Ll. Pérez, A. Lara, D. Casellas, J.M. Prado: *19th European Conference on Fracture (ECF19)*, 2012.
30. O. Akourri, M. Louah, A. Kifani, G. Gilbert, G. Pluvinage: *Eng. Fract. Mech.*, 2000, pp. 491–505.
31. D. Gutiérrez, Ll. Pérez, A. Lara, D. Casellas, and J.M. Prado: *Rev. Metal.*, 2013, vol. 49 (1), pp. 45–54.
32. K. Mori, Y. Abe, and Y. Suzui: *J. Mater. Proc. Technol.*, 2010, vol. 210, pp. 653–59.
33. P. Larour, J. Freudenthaler, A. Grünsteidl, K.Wang: *Proceedings of the IDDRG2014*.
34. M. Kapp: PhD Thesis. Erich Schmid Institute of Materials Science, 2011.
35. H. Mohrbacher: *Adv. Manuf.*, 2013, vol. 1, pp. 28–41.